21st Australasian Fluid Mechanics Conference
Adelaide, Australia
10-13 December 2018

Vortex Rings in a Stratified Fluid

J. Elsnab, M. Zhen, J. Philip and J. Klewicki

Department of Mechanical Engineering
University of Melbourne, Victoria 3010, Australia

Abstract

The motion of vortex rings propagating horizontally in a linearly stratified medium is investigated using time-resolved planar particle imaging velocimetry. The experiments are conducted in a large water tank. Vortex rings are produced using a piston-cylinder apparatus that is driven by a stepper motor. Linear stratification is obtained using a double bucket method described in the literature. The structure and interactions of a vortex ring with a linearly stratified media are determined by the Reynolds and Froude numbers at a fixed formation ratio of the vortex ring generation. These experiments are designed to investigate the effect of varying the aforementioned parameters. The results provide further insight on the effect of stratification on vortex ring evolution, vorticity generation, and ring collapse.

Introduction

Vortex rings have fascinated researchers for nearly 150 years and can be considered the simplest form of more general concentrated vortices, e.g., cyclones. One motivation behind investigating vortex rings interacting with surfaces and other flows stems from observed similarities to the spatially compact coherent motions in turbulent flows. Maxworthy [4] suggests that the mechanisms by which vortex rings entrain fluid is similar to that by which turbulent fluid entrains laminar fluid at a turbulent-laminar interface. Linden [3] used a vortex ring interacting with a density step as a model for plume entrainment and grid generated turbulence. Vortex rings have also been investigated in a linearly stratified medium. In their flow visualization study, Johari and Fang [2] reported that when the internal Froude number was less than 1.3, the ring retained its overall geometry, but continually decreases in size. For Froude numbers greater than 3.2, they reported pronounced asymmetry in the ring geometry. This led to a two-level classification of the collapse process.

Vorticity, $\omega = \nabla \times \mathbf{u}$, has long been purported to be the natural variable for studying turbulent flows. Here $\mathbf{u}$ is the velocity vector, bold quantities represent a vector, and $\times$ denotes the cross-product. Understanding how vorticity is generated is of fundamental importance. In the presence of stratification, the baroclinic torque (BT) term contributes to the generation of vorticity. This term is defined as

$$\frac{1}{\rho^2}\nabla\rho \times \nabla p, \tag{1}$$

where ρ is the density and p is the pressure. Following Johari and Fang, the pressure term can be split into a hydrostatic ($\nabla\rho gy$) and the hydrodynamic components (p'), e..g,

$$\frac{1}{\rho^2}\left(\nabla\rho \times \nabla p' - \rho g \nabla\rho \times \hat{j}\right), \tag{2}$$

where g is the acceleration of gravity and the gravity vector is taken to be along the negative y direction. It is useful to make the vorticity transport equation dimensionless. The ratio of the vortex ring circulation, ζ, to the exit diameter of the vortex tube, D, is the velocity scale, and the corresponding time scale is D^2/ζ. The buoyancy frequency $N = [(-g/\rho_0)d\rho/dy]^{1/2}$ is used to make the density gradient dimensionless, where ρ_0 is the reference density. Lastly, the hydrodynamic pressure is normalized by $\rho_0(\zeta/D)^2$. The dimensionless vorticity transport equation then becomes

$$\begin{aligned}\frac{\mathbf{D}\omega^*}{\mathbf{D}t^*} &= \omega^*\nabla^*\mathbf{u}^* + \left(\frac{\nu}{\zeta}\right)\nabla^{*2}\omega^* \\ &- \left(\frac{DN^2}{g}\right)\frac{1}{\rho^{*2}}\nabla^*\rho^* \times \nabla^* p'^* \\ &+ \left(\frac{N^2D^4}{\zeta^2}\right)\frac{1}{\rho^*}\nabla^*\rho^* \times \hat{j}, \end{aligned} \tag{3}$$

where the superscript $*$ represents dimensionless variables.

Equation 3 contains the following dimensionless parameters: circulation-based Reynolds number, $Re = \zeta/\nu$ (ν is the kinematic viscosity); the ratio of stratification length scale to the flow length scale, $g/(DN^2)$; and the Froude number, $Fr = \zeta/(ND^2)$. The hydrostatic BT term is dominant when the Fr is order unity while the Re and $g/(DN^2)$ are much greater than Fr. In this case, viscous diffusion and hydrodynamic BT terms are smaller than the hydrostatic BT term. The flow length scale, D, is always smaller than the stratification length scale g/N^2, therefore, the term containing DN^2/g is negligible. As such, Fr is the most significant dimensionless parameter affecting the vortex ring influenced by stratification.

The objective of this study is to investigate the effect of linear stratification on a vortex ring and the generation of vorticity through the BT term in the vorticity transport equation by varying the Fr and Re. These effects are discerned using time-resolved particle imaging velocimetry (PIV).

Experiment Description

Experimental Facility and Stratification

Vortex rings are generated using a piston-cylinder device and a D = 34.8 mm seamless tube. The cylinder and tube are connected using flexible tubing. The piston-cylinder motion is precisely controlled using a stepper motor. A vortex ring is produced at the exit of the tube by converting rotational motion from the stepper motor to translation using a threaded rod. Trapezoidal velocity versus time profiles are implemented in LabView with an impulse configuration, i.e., acceleration time is much less than the overall time interval, T. The vortex generator is used in a water tank with width of 1.1 m, length of 3.6 m and height of 0.37 m. The glass tank is filled with water maintained at a constant water level to ensure constant hydrostatic pressure. Vortex rings are formed using a stroke length, L/D of 1.5, where L is the fluid displacement in the tube.

In order to obtain a linear stratification within the experimental tank, a variant of the Osters [5] double bucket method is used.

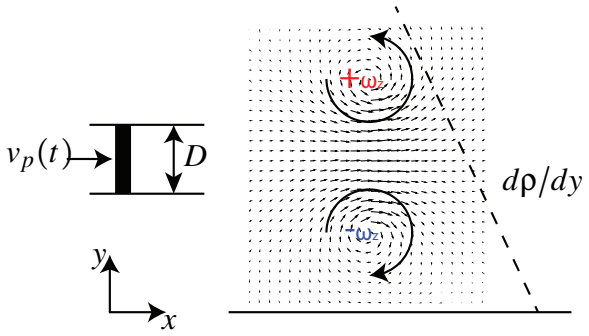

Figure 1: A schematic of a vortex ring in a linearly stratified fluid. The spanwise vorticity is ω_z, D is the diameter of the vortex ring generation tube, $v_p(t)$ is the velocity of the piston as a function of time, and $d\rho/dy$ is the density gradient.

In the usual double bucket method, fluid of varying density is injected from the top of the experimental tank through a float system. For this study, it is more convenient to fill the experimental tank from the bottom starting with low density fluid followed by increasing density fluid. Initially, the supply tank contains heavy fluid while the mixing tank contains only light fluid. Once the filling process starts, heavy fluid flows from the supply tank to the mixing tank where it mixes with the lighter fluid increasing the density of the latter fluid. As time advances, the density of the fluid contained in the mixing tank increases. In order to improve mixing and increase homogeneity, a stirring device is used in the mixing tank. The well mixed fluid is distributed along the bottom of the vortex ring facility using four diffusers. The density gradient is determined by sampling the mixture at various heights and determining the density using a pycnometer and precision mass balance. Two locations are sampled to ensure that the density gradient is invariant in horizontal planes. The vortex ring interaction with the density gradient is schematically shown in figure 1.

Data Acquisition and Reduction

PIV data are obtained at the wall-normal plane of symmetry (xy plane). A 5 W continuous laser is used as the light source and PIV images are acquired using a high-speed CCD camera with resolution 2000 by 2000 pixel^2. The water tank is seeded with silver-coated particles nominally 15 μm in diameter. The time delay between image capture ranges from 3 – 6.5 ms so that the maximum displacement of the vortex ring ranges from 8 – 10 pixel. Note that index matching was not used for these experiments due to the low salt concentration.

For post processing of the PIV images, a multi-pass, multi-grid, cross-correlation algorithm is utilized [1]. A base interrogation window size of 64 by 64 pixel^2 is used for the first pass, which is subsequently followed by a window size of 32 by 32 pixel^2 with 50% overlap in the second pass. The field of view (FOV) starts $2/3D$ from the vortex generation tube and the centreline of the tube is $2.0D$ from the floor in the wall-normal direction for all cases investigated. The PIV FOV is $3.4D$ by $3.4D$ and is centred on the wall-normal plane of symmetry of the ring. The spatial resolution of velocity vectors in both the streamwise and wall-normal directions is $0.031D$. The spanwise vorticity, ω_z, is obtained by differentiating the velocity field using a least-squares method. The circulation, ζ, in the upper and lower half of the ring is obtained by Stokes theorem, $\oint u \cdot \mathbf{d}l = \int \omega_z \mathbf{d}A$, using a two-dimensional version of the trapezoidal rule.

Results

Contour plots of the spanwise vorticity are presented in figures 2 – 5. The circulation for the Re is obtained using a slug model, where the average slug velocity, $\overline{V_s} = 1/T \int v_p(t)dt$ and $1.5D$ is used as the characteristic length. The parameter space investigated satisfies the assumption that the hydrostatic pressure is much larger than the hydrodynamic pressure. For pure water (figure 2), as expected, the contours remain coherent and and are symmetric about $y/D = 2.0$. The BT is maximum when the density gradient is perpendicular to the pressure gradient. Initially, both gradients are in the vertical direction, i.e., no vorticity generation will occur. Therefore, in order for vorticity to be generated, $\nabla\rho$ direction should be at an angle other than 0° or 180° to $\hat{j}$. The constant density lines are tilted by the vortex, resulting in a tilting of the vector $\nabla\rho$ from its stationary direction of $\hat{j}$. This tilting introduces the gradients required for vorticity generation to occur. Density gradients are also potentially introduced during the formation of the ring since the fluid in the vortex tube mixes during the generation process. In figure 3, there is minimal vorticity generation in comparison to figure 4 for the same formation Re number. If the Re is too high, there is no vorticity generation. Results for $Re = 5800$ and $Fr = 5.19, 6.15$, not shown, do not show vorticity generation. Decreasing the Fr at $Re = 2200$ shows additional vorticity generation as shown in figure 5. Note, however, that the symmetry in the terms of the contour shapes remains for all cases. This is not consistent with the findings of Johari and Fang [2], but is in agreement with those of von Atta and Hopfinger [6].

Since interesting physics occur for a Fr decrease from 2.36 to 1.99 at a fixed $Re = 2200$, additional analysis is performed for these cases. The trajectory of the vortex cores, i.e., locations of the minimum and maximum ω_z, shown in figure 6 indicate that stratification decreases the distance between the cores and also indicate that there is no increase or decrease in the vertical direction, i.e., the ring propagates horizontally. Even though there is a linear density gradient, there is no imbalance in the ring. As a result, the vorticity generated due to the baroclinic torque is symmetric. This is consistent since the hydrostatic pressure and density gradients are constant.

The circulation for the bottom and top of the ring are shown in figure 7 where the integration domain is based upon the halfway distance between the vortex cores and is sufficiently sized so that all vorticity values above a threshold are included. The circulation for pure water flows remains nearly constant for this FOV. The data indicate that there is a significant reduction in the circulation for the stratified flows and the upper and lower circulations are equal in magnitude. For $Fr = 1.99$, there is a cross-over point at $x/D = 2.5$ where the overall circulation switches sign, but the ring has not collapsed for this FOV.

The minimum and maximum ω_z for the top and bottom cores are shown in figure 8. For the pure water scenario, the minimum and maximum decay owing to diffusion. Increasing the stratification further reduces these values. For the pure water scenario, the minimum and maximum ω_z decrease linearly, whereas for $Fr = 0.1.98$ and $Fr = 2.36$ scenarios the decay starts off linear and then approaches a constant.

Conclusion

Vortex ring evolution under the influence of a linearly stratified environment were investigated. The results indicate that the ring remains symmetric for all Fr and Re investigated. Vorticity due to the BT was generated if the $Re < 2950$, and there was no evidence of the ring collapsing for this Fr range.

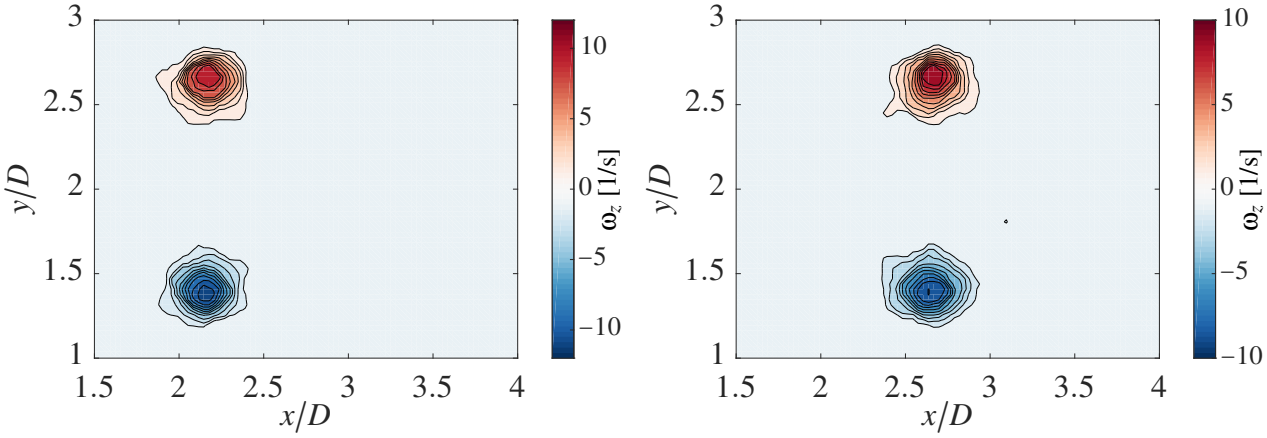

Figure 2: Contours of the spanwise vorticity for pure water at $Fr = 0$ and $Re = 2200$.

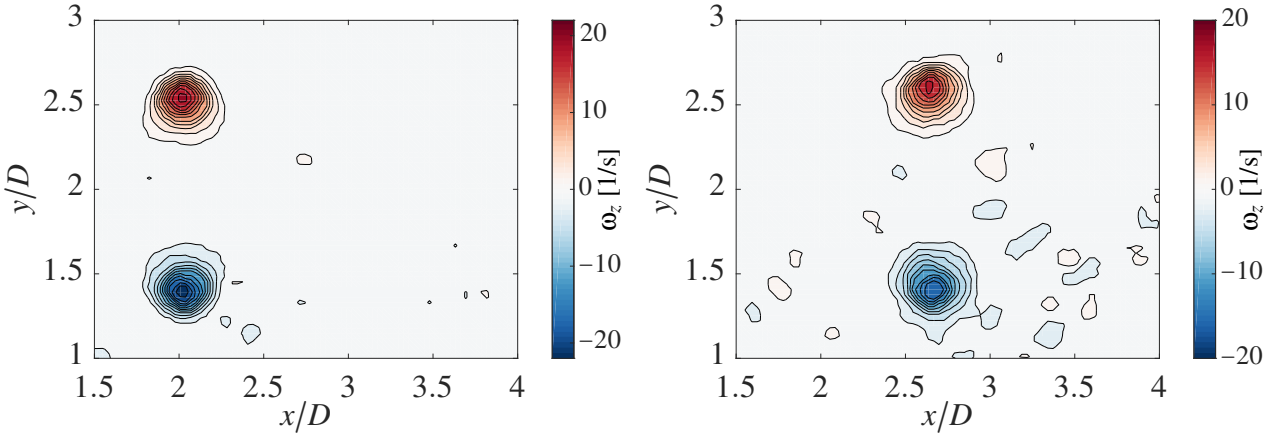

Figure 3: Contours of the spanwise vorticity for stratified flows at $Fr = 3.12$ and $Re = 2950$.

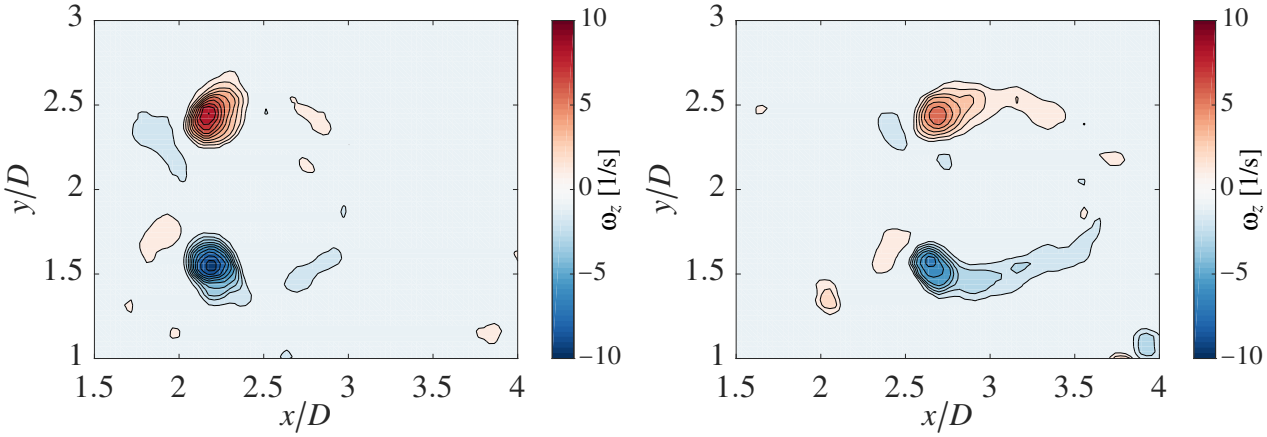

Figure 4: Contours of the spanwise vorticity for stratified flows at $Fr = 2.36$ and $Re = 2200$.

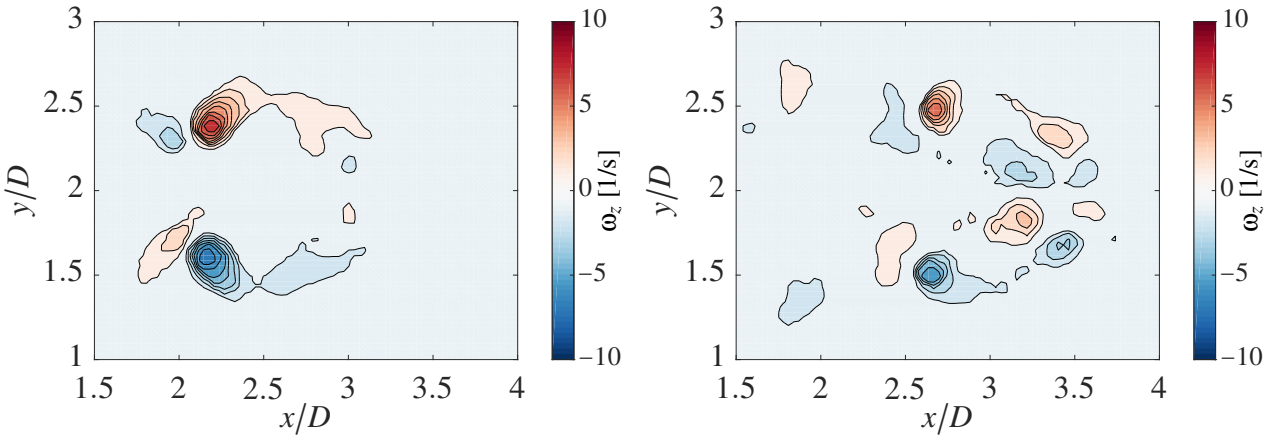

Figure 5: Contours of the spanwise vorticity for stratified flows at $Fr = 1.99$ and $Re = 2200$.

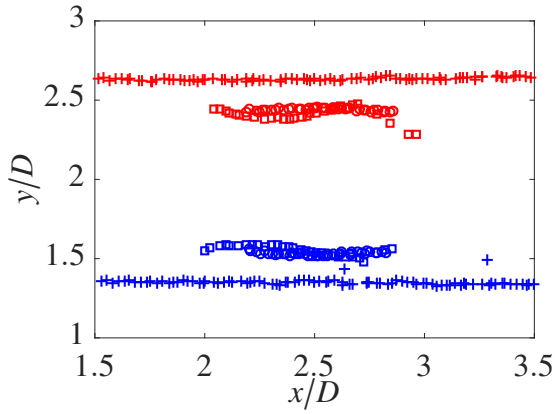

Figure 6: Trajectory of the minimum and maximum spanwise vorticity. Description: +, $Re = 2200$, $Fr = 0$; ∘, $Re = 2200$, $Fr = 2.36$; and □, $Re = 2200$, $Fr = 1.99$.

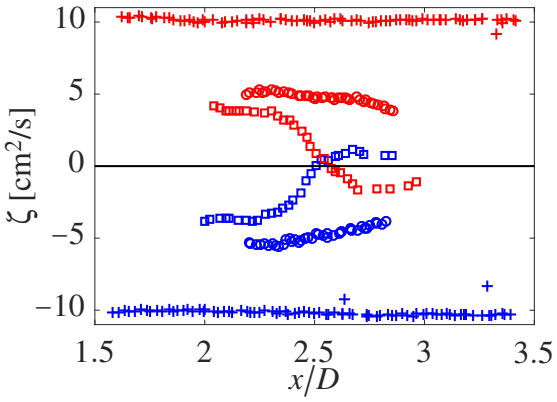

Figure 7: Circulation for the top and bottom half of the vortex ring. Description: +, $Re = 2200$, $Fr = 0$; ∘, $Re = 2200$, $Fr = 2.36$; and □, $Re = 2200$, $Fr = 1.99$

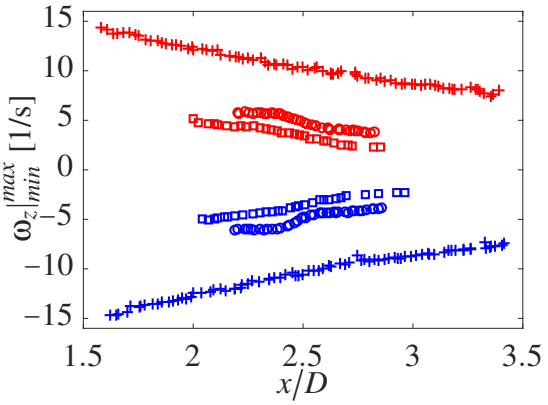

Figure 8: Minimum and maximum spanwise vorticity of the vortex ring. Description: +, $Re = 2200$, $Fr = 0$; ∘, $Re = 2200$, $Fr = 2.36$; and □, $Re = 2200$, $Fr = 1.99$

References

[1] Adrian, R. J. and Westerweel, J., *Particle image velocimetry*, Cambridge University Press, 2011.

[2] Johari, H. and Fang, H., Horizontal vortex ring motion in linearly stratified media, *Physics of Fluids*, **9**, 1997, 2605–2616.

[3] Linden, P. F., The interaction of a vortex ring with a sharp density interface: a model for turbulent entrainment, *Journal of Fluid Mechanics*, **60**, 1973, 467480.

[4] Maxworthy, T., The structure and stability of vortex rings, *Journal of Fluid Mechanics*, **51**, 1972, 1532.

[5] Oster, G., Density gradients, *Scientific American*, **213**, 1965, 70–79.

[6] Van Atta, C. and Hopfinger, E., Vortex ring instability and collapse in a stably stratified fluid, *Experiments in fluids*, **7**, 1988, 197–200.